*Original*

Silva Campos, M.R.; Scharnagl, N.; Blawert, C.; Kainer, K.U.:

**Improving corrosion resistance of Mg10Gd alloy**

Materials Science Forum, Light Metals Technology Conference, LMT 2013 (2013)
Trans Tech Publications

DOI: 10.4028/www.scientific.net/MSF.765.673

*Materials Science Forum* *Online: 2013-07-31*
*ISSN: 1662-9752, Vol. 765, pp 673-677*
*doi:10.4028/www.scientific.net/MSF.765.673*


# Improving Corrosion Resistance of Mg10Gd Alloy

Maria del Rosario Silva Campos[a], Nico Scharnagl[b], Carsten Blawert[c] and Karl Ulrich Kainer[d]

Institute of Materials Research, Helmholtz-Zentrum Geestacht Centre for Materials and Coastal Research, Max-Planck-Str. 1, 21502 Geesthacht, Germany

[a]maria.silva@hzg.de, [b]nico.scharnagl@hzg.de, [c]carsten.blawert@hzg.de, [d]karl.kainer@hzg.de

**Keywords:** Magnesium corrosion, Rare-earth Gd, Mn additions, EIS

**Abstract.** In a screening test, typical traditional alloying elements for magnesium (Al, Mn, Zn, Y) were added to Mg10Gd alloy to study their influence on its corrosion resistance. The Mg10Gd1Mn alloy was identified as the most promising ternary alloy system. While addition of Gd alone disturbs the passive film formation the presence of Mn is beneficial for recovery of the passivity. Performance of the Mg10Gd1Mn alloys is comparable to high purity Mg.

## Introduction

Corrosion of magnesium alloys continues to be a major technological issue [1]. Important improvements have been achieved during the last decade in increasing the resistance of magnesium alloys against corrosion in the presence of chloride containing environments. The introduction of "high purity" Mg alloys with low heavy metal impurity (Ni, Cu, and Fe) level has reduced their corrosion rate by about two orders of magnitude when measured by immersion test in NaCl solutions [2-4]. The NaCl solution favours anodic magnesium oxidation, but the presence of rare earth elements improves the tendency of magnesium to passivation. The dissolution rate in chlorides is higher, because chlorides can interfere with the formation and maintenance of a protective layer of corrosion products which decrease the severity of the attack [5]. Magnesium alloys show strong susceptibility to localized corrosion in chloride solutions due to their inhomogeneous microstructure. The existence of intermetallics in the microstructure alloys might represent initiation sites for localized corrosion. This is due to the formation of galvanic couples between the intermetallics and the surrounding matrix [6]. However, the casting conditions and subsequent heat treatment in some cases are also important factors which influence both the corrosion rate and morphology of attack [7-8]. Among Mg alloys, the most common are those alloyed with Al and Mn (e.g. AM50 and AM60) and with Al and Zn (e.g. AZ91) whose mechanical properties and corrosion behaviour are well established [5]. Nevertheless, it has been observed that addition of RE elements to magnesium alloys improves their corrosion resistance [9]. The aim of this work is to compare and understand the changes in corrosion behaviour when pure Mg is alloyed with Gd (Mg10Gd) and Gd-Mn (Mg10Gd1Mn).

## Experimental Procedures

**Materials.** Pure Mg specimens were directly tooled from commercial HP Mg ingots. The Mg10Gd and Mg10Gd1Mn alloys were prepared from the pure elements. Pure magnesium was melted using an electrical resistance furnace under protective atmosphere of Argon-SF6 and the alloying elements were added at temperatures between 680-700 °C. The final alloys were cast into a cylindrical steel mould (gravity die casting). After casting, the chemical composition of each cast bar was measured at the top and bottom positions in order to ensure compositional homogeneity in the whole specimen using X-ray fluorescence (XRF) see Table 1.

**Microstructure and Composition.** Top views of the specimen were prepared by standard metallographic techniques. The microstructure and composition of the phases was studied using a ZEISS Ultra 55 scanning electron microscope equipped with an energy-dispersive X-ray analysis system (EDX).The acceleration voltage was ranging from 8-20 keV.

**Electrochemical Evaluation.** Specimens with dimensions 15 mm diameter x 5 mm thickness were ground with SiC paper up to grit 1200, ultrasonically cleaned using ethanol and finally dried in hot air. Electrochemical tests were performed using a three electrode cell with 330 ml electrolyte volume. The specimen is the working electrode (WE) with a ~0.5 $cm^2$ exposed area, while reference (RE) and auxiliary (AE) electrodes were Ag/AgCl, and Pt grid respectively. The electrolyte was a stirred aqueous solution of 0.5 mass% NaCl at room temperature (21.5 ± 0.5 °C). The cell was connected to a Gill AC Potentiostat from ACM Instruments. The sequence of measurements started with 30 minutes open circuit potential (OCP) followed by potentiodynamic polarisation measurement starting at -150 mV relative to the free corrosion potential. The scan rate was 12 mV/min and the test was terminated when a current limit of 0.1 mA/$cm^2$ was exceeded. Electrochemical impedance spectroscopy (EIS) measurements were performed using a frequency range between $10^{-2}$ and $10^4$ Hz and ± 10 mV amplitude. These measurements were repeated after different exposure periods of 1, 3, 6, 12, 24, 48, 72, 96, 120 and 144 h. All the above-mentioned measurements were performed in triplicate to guarantee the reliability of the results.

## Results and Discussion

**Microstucture.** Fig. 1 shows a typical dendritic as cast microstructure of Mg10Gd1Mn. Primary Mg dendrites are visible with Gd rich secondary Mg and $Mg_5Gd$ intermetallic between the dendrite arms. EDX quantitative analyses were done in the 4 different regions identified as a, b and c (see Table 2). It is possible to observe Mn in solid solution in the matrix and the intermetallics.

Table 1. Chemical analysis of the alloys.

| | Top [wt.%] | | Btm. [wt.%] | | |
|---|---|---|---|---|---|
| | Gd | Mn | Gd | Mn | Bal |
| Mg10Gd | 9.05 | - | 8.97 | - | Mg |
| Mg10Gd1Mn | 8.69 | 1.03 | 8.83 | 1.02 | Mg |

Table 2. EDX quantitative analysis of Mg10Gd1Mn.

| | a [at.%] | b [at.%] | c [at.%] |
|---|---|---|---|
| OK | 0.6-0.95 | 0.17 | 0.61 |
| MgK | 87-92 | 99 | 95 |
| SiK | 0.11-0.15 | 0.06 | 0.07 |
| MnK | 0.29-0.56 | 0.02 | 0.34 |
| GdK | 7-10 | 0.76 | 3.33 |

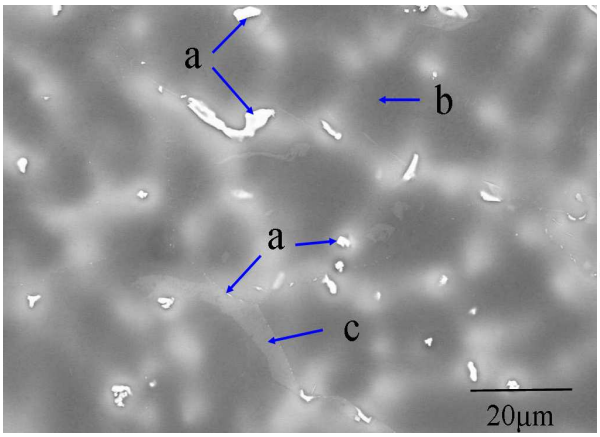


Fig. 1. SEM micrograph of Mg10Gd1Mn.

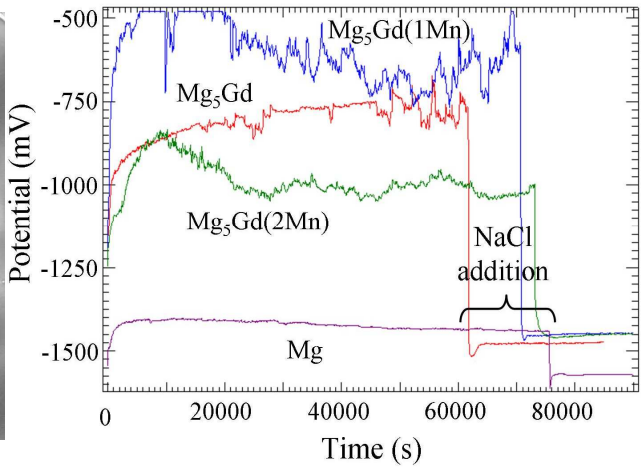


Fig. 2. OCP vs. immersion time and sodium chloride addition (0.5%) for Mg pure, Mg10Gd and Mg10Gd1Mn.

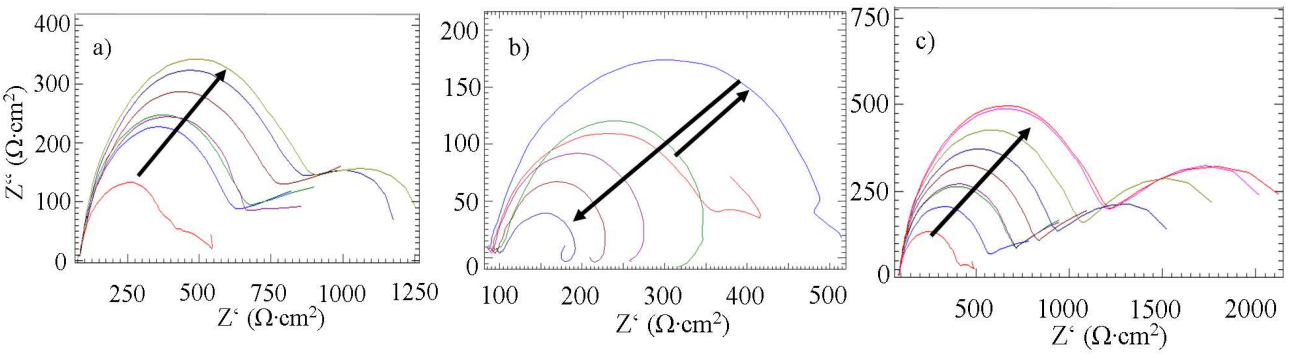


Fig. 3. Nyquist plots for Mg pure, Mg10Gd and Mg10Gd1Mn as a function of immersion time in aerated aqueous 0.5% NaCl solution.

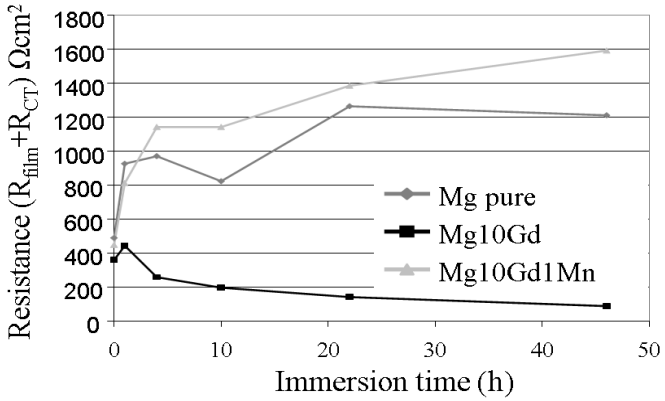


Fig. 4. Comparison of the sum of passive film and charge transfer resistance for the three alloys as a function of immersion time in 0.5% NaCl solution.

Table 3. Composition of the surface oxide layer on the three alloys after impedance testing in 0.5% NaCl determined by EDX analysis.

| Alloy/Elem. [at %] | Mg | Gd | O | C | Mn |
|---|---|---|---|---|---|
| Mg pure | 31 | - | 53 | 15 | - |
| Mg10Gd | 27-28 | 0.1-0.2 | 54-60 | 10-11 | - |
| Mg10GdMn | 16-29 | 3-8 | 47-52 | 17-20 | 1-1.5 |

**Corrosion Behaviour.** Fig. 2 shows the free corrosion potential of the intermetallic phase $Mg_5Gd$ (pure and with 1 and 2 wt% Mn in solid solution) and pure Mg in deionised water. In water, the intermetallic phase is less stable than pure Mg, which is reflected by larger potential variations. Smaller additions of Mn seem to increase the free corrosion potential of the $Mg_5Gd$ phase, while larger amounts have the opposite effect. However, all potentials of the intermetallics are much nobler than the potential of pure Mg, but the dissolution of the intermetallic phases is faster compared to pure Mg. The dissolution of the intermetallics dramatically increases if NaCl is added to the deionised water and the negative effect is also visible in the large drop of the free corrosion potential which is much closer to the potential of Mg after chloride ions are present. This is also consistent with the corrosion rates determined from potentiodynamic polarisation measurements in millimetres per year, mm/y (Mg: 0.58 ± 0.15, $Mg_5Gd$: 7.41 ± 0.47, $Mg_5Gd$(1Mn): 9.98 ±2.28 and $Mg_5Gd$(2Mn): 10.86 ± 2.69). Thus one can assume that intermetallics are cathodic to the matrix, but the question is if the dissolution of Mg (sacrificial anode) is fast enough to prevent the dissolution of the intermetallics. Differences in potential between pure $Mg_5Gd$ and those containing Mn are not large but the corrosion resistance is largely affected. Impedance results shown in Figs. 3 & 4 reveal the corrosion performance of pure Mg and the two alloys in 0.5% NaCl solution. The alloys can be considered a combination of a Mg matrix and intermetallics distributed randomly in the matrix. The only difference is the fact that Gd not only forms the intermetallic with Mg but is also in solid solution in

the matrix, and Mn is not only found in solid solution in the intermetallics but also in the Mg matrix. Due to the absence of galvanic effects, the corrosion performance of pure Mg is expected to be the best. This good corrosion performance is indeed demonstrated in Fig. 3a and the binary Mg10Gd alloy shows the expected poorer corrosion performance (Fig. 3b). Interestingly the performance of the Mg10Gd1Mn alloy is even better than that of pure Mg (Fig. 3c), which indicates, how important the passive (protective) film formation for Mg alloys can be. Right after immersion, the impedance spectra (Fig. 3) are more or less the same for all three materials with some instability at lower frequencies, probably indicating some localised dissolution. After one-hour immersion, corrosion resistance is still increasing for all three materials, but for the Mg10Gd alloy the low frequency instabilities are becoming dominant, while for the other two materials, the passive film formation is dominating. For the remaining immersion time up to 46 hours the pitting is further increased and the corrosion resistance is decreased for the Mg10Gd alloy, while the pure Mg and the Mg10Gd1Mn alloy reveal an increasing passive film thickness without any sign of localised corrosion, resulting in continuously increasing corrosion resistance values (Fig. 4), which can be related to the increasing thickness of the passive film. The performance of the Mg10Gd1Mn alloy is better than that of pure Mg, which can be related to faster and passive film formation with higher thickness.

**Passive Film Morphology and Composition.** Non-destructive thickness measurements using eddy currents performed right after the corrosion test revealed the following thicknesses for corrosion products on the surface of the specimens: pure Mg: 16 µm < Mg10Gd1Mn: 50 µm < Mg10Gd: 150 µm. This is more or less consistent with the SEM observation of surface morphology of the films (Fig. 5). The film on pure Mg appears to be compact and dense (Fig. 5a) and the visible cracks are most likely a result of drying of the film after the specimens were taken out of the electrolyte (Fig. 5b). The adhesion of the film is nevertheless good and no flaking off can be observed. Most of the surface is covered by a flat and compact oxide layer (Fig. 5d) and only small regions have a needle-like appearance (Fig. 5c). The needles or plates are small and a compact layer seems to be located underneath them. It is likely that the needles are indicating accelerated dissolution and deposition of $Mg(OH)_2$/MgO while the compact modification is a result of slow dissolution and deposition. In contrast, the adhesion of the corrosion products is poor for the Mg10Gd alloy and the first flaking off can already be observed during thickness measurements. This poor adhesion is obviously related to the almost 10 times thicker film compared to the pure Mg. Fig. 5e shows some film remains on the surface and a more detailed view shows the whole surface covered by very coarse needles/plates, not forming a dense and compact film. The dissolution is obviously so fast that the compact film formation is suppressed and no protective film is formed. If manganese is added, the dissolution rate is reduced again and although the film is still thicker compared to pure Mg it still has reasonable adhesion to the substrate. Due to the greater thickness, cracking is more severe and some flaking off can be observed (Fig. 5h). However, similar to pure Mg most of the film is still compact (Fig. 5j) and in regions of higher dissolution needles can be observed which have similar size compared to those observed on pure Mg (Fig. 5i). A compact film is also visible underneath it. The EIS results confirm that in the electrolyte the film is compact, protective and that the cracking is only a problem of the dry film. Considering the composition of the various films determined by EDX analysis (Table 3), it is clear that the film on pure Mg is mainly composed of MgO/$Mg(OH)_2$ with some fraction of $MgCO_3$. The carbonate can form from $CO_2$ dissolved in the aqueous electrolyte. The film on Mg10Gd has a very similar composition and Gd is almost not present in the film formed by the corrosion products. Mainly Mg is the dominating film forming element indicating that it dissolves quicker than the Gd which may remain in the alloy or at the interface to the corrosion product film. The carbonate fraction appears to be reduced as well. Adding 1 wt% of manganese completely changes the behaviour. There is a clear enrichment of Gd and Mn in the passive film, indicating that Mg dissolves slower and dissolution of Gd (intermetallics) is enhanced. Nonetheless the main components are still MgO/$Mg(OH)_2$, obviously with an increasing content of carbonate (carbon concentration is increasing as well). From the EDX result one can only speculate if the additional Gd and Mn detected are responsible for the increasing carbonate fraction or if they contribute to the oxide/hydroxide fraction.

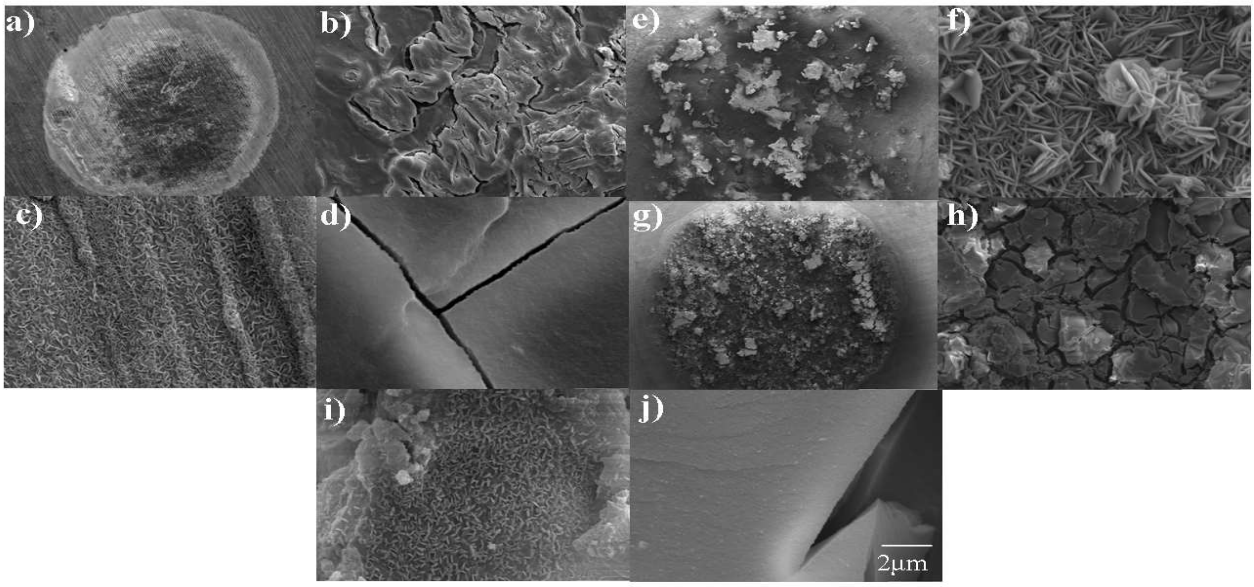


Fig. 5. Surface morphology of pure Mg (a, b, c, d), Mg10Gd (e, f) and Mg10Gd1Mn (g, h, i, j) after impedance testing in 0.5% NaCl solution.

## Summary

Additions of Mn improve the corrosion resistance of Mg10Gd alloy. Mn is found in solid solution in the matrix and the Mg5Gd intermetallics, without forming theri own compounds. Thus it may be available for passive film formation reducing the negative effects of the Gd addition. This observation gives an idea how important the formation of the passive layer on the surface of Mg alloys is for reducing the corrosion rate.

## References

[1] N. Birbilis, M.A. Easton, A.D. Sudholz, S.M. Zhu, M.A. Gibson, On the corrosion of binary magnesium-rare earth alloys, Corr. Sci. 51 (2009) 683-689.

[2] K. Nisancioglu, O. Lunder, T.K. Aune, Corrosion mechanism of AZ91 magnesium alloy, in: 47th Annual World Magensium Conference, Cannes, 1990, pp. 43.

[3] W.E. Mercer, J.E. Hillis, The critical contaminant limits and salt water corrosion performance of magnesium AE42 alloy, in: SAE Technical paper No. 920073, 1992.

[4] K.N. Reichek, K.J. Clark, J.E. Hillis, Controlling the salt water corrosion performance of magnesium AZ91 alloy, in: SAE Technical paper No. 850417, 1985.

[5] F. Zucchi, V. Grassi, A. Frignani, C. Monticelli, G. Trabanelli, Electrochemical behaviour of a magnesium alloy containing rare earth elements, J. Appl. Electrochem. 36 (2006) 195-204.

[6] G. Ben-Hamu, D. Eliezer, K.S. Shin, The role of Si and Ca on new wrought Mg–Zn–Mn based alloy, Mat. Sci. Eng. A 447 (2007)35-43.

[7] O. Lunder, K. Nisancioglu, T.K. Aune, Corrosion of cast magnesium-aluminium alloys, in: Proceedings of International Coference on Recent Advances in Science and Engineering of Light Materials, Sendai, Japan, 1991, pp. 157.

[8] T.K. Aune, Minimizing base metal corrosion on magnesium products: the effect of element distribution (structure) on corrosion behavior, in: International Magnesium Association, Toronto, Canada, 1993.

[9] L.L. Rokhlin, Magnesium Alloys Containing Rare Earth Metals: Structure and Properties, Taylor & Francis, 2003.